# Dynamic behaviour of SO₂ and NO ligands in hexanuclear ruthenium clusters as probed by ¹H NMR signals of a coexisting μ-allyl ligand ‡

**Teiji Chihara, Aldo Jesorka, Hidenori Ikezawa and Yasuo Wakatsuki** *,†

*The Institute of Physical and Chemical Research (RIKEN), Wako-shi, Saitama 351–01, Japan*

A hexanuclear ruthenium carbide carbonyl cluster with SO₂ and μ-η³-C₃H₅ ligands, [Ru₆C(CO)₁₄(SO₂)(μ-η³-C₃H₅)]⁻ shows fluxionality with $\Delta H^{\ddagger} = 7.3$ kcal mol⁻¹ and $\Delta S^{\ddagger} = -16.6$ cal K⁻¹ mol⁻¹ as observed by variable-temperature ¹H NMR spectroscopy of the *syn*- and *anti*-protons of the μ-η³-C₃H₅ moiety. Likewise, fluxionality of a neutral cluster complex with NO and allyl groups, [Ru₆C(CO)₁₄(NO)(μ-η³-C₃H₅)], has been found to have $\Delta H^{\ddagger} = 9.5$ kcal mol⁻¹ and $\Delta S^{\ddagger} = -7.8$ cal K⁻¹ mol⁻¹. The 2-methoxycarbonylallyl analogue of [Ru₆C(CO)₁₄(NO)(μ-η³-C₃H₄CO₂Me)], exhibits similar fluxional behaviour with virtually identical parameters ($\Delta H^{\ddagger} = 9.2$ kcal mol⁻¹ and $\Delta S^{\ddagger} = -7.1$ cal K⁻¹ mol⁻¹), while model analysis based on its single-crystal structure indicates that rotation of the η³-co-ordinated allyl group would have a very high steric barrier. The observed dynamic behaviour was thus concluded to arise from rapid migration of the SO₂ or NO ligand over the metal atoms in the cluster core.

The fluxional behaviour of ligands in cluster complexes has attracted attention as a model for the movement of chemisorbed small molecules on metal surfaces. In this context the mobility of ligands on a large cluster core appears particularly interesting and a number of reports has described the dynamics of clusters with five, six, and even higher nuclearities. Most of the fluxionality in these high-nuclearity clusters is concerned with carbonyl scrambling and/or hydride shift on the cluster cores,[1] but dynamic processes of other ligands have also been noted, for example Cu{P(C₆H₁₁)₃},[2] Au(PPh₃),[3] benzyne,[4] vinylidene,[5] SMe[5] and PPh₂.[6] A problem in large-cluster systems is the presence of many ligands or complexity of the NMR spectra which prevents detailed analysis; precise simulation and elucidation of the activation parameters have been reported for trinuclear clusters[7] but very seldom for clusters with higher nuclearity.

We have been investigating the fixation of air-polluting gases on hexanuclear ruthenium carbonyl clusters. Since one of the promising processes for removing NO from diesel engine exhaust is reduction by hydrocarbons on a supported metal surface,[8] we have prepared ruthenium carbonyl clusters with allyl/NO and allyl/SO₂ ligands, regarding the allyl group as a model for a chemisorbed hydrocarbon.[9] The solid-state structures and the relative orientation of allyl/NO or allyl/SO₂ have been determined by X-ray crystallography. Although we have been unable to detect any discrete product on heating, which may be formed by the reaction of the allyl ligand with co-co-ordinating NO or SO₂ at elevated temperatures, the fluxionality of the complexes at lower temperatures was notable. The presence of a μ-allyl ligand has been found to be particularly useful for the analysis of fluxional behaviour because the signals due to protons at the allyl terminal carbons can easily provide information if the left and right halves of the cluster are magnetically equivalent.

In this paper we report variable-temperature NMR spectra of four ruthenium cluster complexes and simulations of allyl-proton signals which supply activation parameters corresponding to the mobility of NO and SO₂ ligands on the hexanuclear cluster core. In a previous communication we suggested the possibility of allyl group rotation in one of the allyl/NO clusters,[10] but a detailed study using a substituted allyl ligand described here is compatible with a stationary allyl group and migrating NO ligand. To the best of our knowledge the present report represents the first example of NMR observations of dynamic processes brought about by migration of NO and SO₂ in large cluster complexes.

## Results and Discussion

### [N(PPh₃)₂]₂[Ru₆C(CO)₁₅(SO₂)] 1

We first examined the variable-temperature ¹³C NMR spectra (400 MHz) of [N(PPh₃)₂]₂[Ru₆C(CO)₁₅(SO₂)] **1**[11] in CD₂Cl₂, the structure of which was expected to be similar to that of the iron analogue,[12] *i.e.* with the SO₂ ligand in a bridging position. At 183 K two peaks were observed, a very broad peak centred at about δ 211 and a sharper peak at δ 202.5 (Fig. 1). From the peak intensities the low-field peak may be assigned to carbonyls co-ordinating to the two metal atoms which are bridged by the SO₂, while the high-field peak is due to the rest of the CO groups. The two peaks coalesce at 213 K and become a sharp single peak (δ 207.7) above 273 K, indicating facile scrambling of the CO ligands even at −60 °C. As discussed in the following section, SO₂ in **1** is also expected to begin its migration above *ca.* −20 °C.

### [N(PPh₃)₂][Ru₆C(CO)₁₄(SO₂)(C₃H₅)] 2

The crystal structure of compound **2**, which we report in detail elsewhere,[11] has the anionic part shown. The allyl group bridges one of the equatorial Ru–Ru bonds while SO₂ bridges the equatorial–apical Ru–Ru edge away from the allyl-co-ordinating metal bond: the molecule has, therefore, no symmetry.

The ¹H NMR spectrum (400 MHz) measured at 193 K exhibited two different *anti*-protons as doublets at δ 0.09 ($J = 12.7$) and 0.47 ($J = 11.6$ Hz), a multiplet for the central proton at δ 1.57, and a multiplet of *syn*-protons at δ 3.87 (Fig. 2). As the temperature is raised the *anti*-proton peaks coalesce at 253 K to a broad singlet: Fig. 2 shows comparisons with computer-generated spectra for the permutation of the *anti*-protons which yield activation parameters (Fig. 5) $\Delta H^{\ddagger} = 7.3 \pm 0.8$ kcal mol⁻¹ and $\Delta S^{\ddagger} = -16.6 \pm 3.2$ cal K⁻¹ mol⁻¹. Since the two *syn*-proton signals overlap and the simulation is valid only for the well separated *anti*-proton peaks, the standard deviations of the parameters obtained are much larger than those for compounds **3** and **4** where both *syn*- and *anti*-protons are simulated (see below).

† E-Mail: waky@postman.riken.go.jp
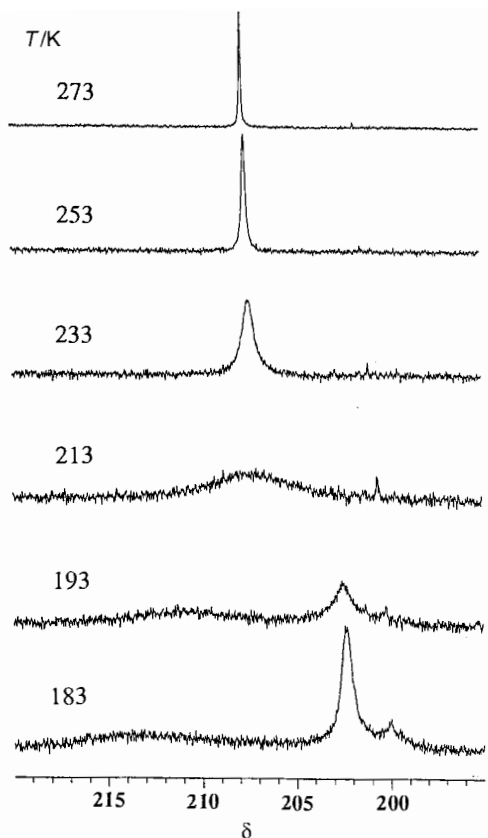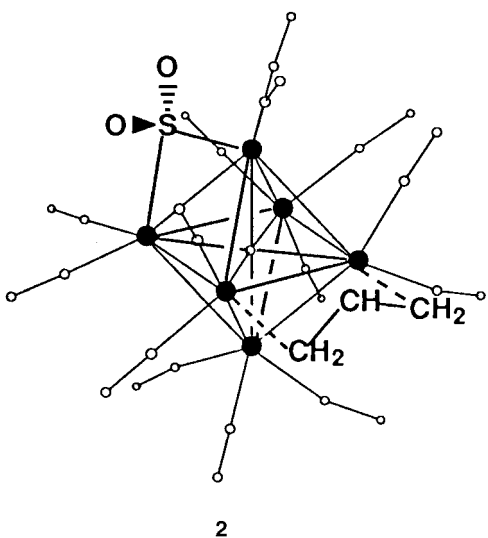‡ *Non-SI unit employed:* cal = 4.184 J.

**Fig. 1** Variable-temperature $^{13}$C NMR spectra (400 MHz) of the carbonyl region of compound **1** in $CD_2Cl_2$



**Fig. 2** Variable-temperature $^1$H NMR spectra (400 MHz) of the $C_3H_5$ region of compound **2** in $CD_2Cl_2$. Left: observed spectra. Right: simulated spectra (*syn*- and *anti*-protons only) and rates



**2**



**3**

Two general factors may be considered in order to explain the observed magnetic equivalence of the allyl protons: movement of the allyl group and that of the $SO_2$ ligand. By movement of the allyl ligand itself, however, it is apparently difficult to explain the observed permutation of two *anti*-protons either by $\pi \longrightarrow \sigma \longrightarrow \pi$ rearrangement or by rotation of the allyl group provided that the allyl and $SO_2$ ligands still occupy the original co-ordination sites: the $\pi \longrightarrow \sigma \longrightarrow \pi$ rearrangement will result in equivalence of *syn*- and *anti*-protons on a given carbon, while rotation of the allyl group will never lead to permutation of any protons of the allyl group because the molecule has no symmetry. The second mechanism which is consistent with the present observation is a stationary allyl group and migration of the $SO_2$ ligand over the cluster core, or at least over four edges which do not contain Ru atoms bearing the allyl carbons. Edge-to-edge migration of the $SO_2$ probably can pro-
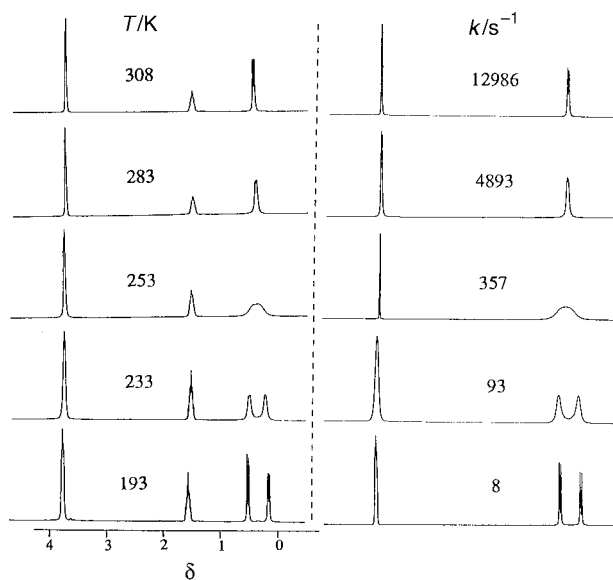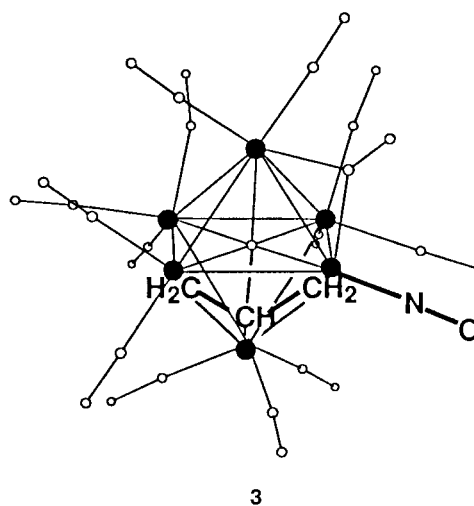
ceed *via* intermediacy of terminally-co-ordinated $SO_2$, well known for mononuclear complexes,[13] or *via* a $\mu_3$-$\eta^2$ configuration as observed in a triiron cluster.[14] The carbonyl ligands are also expected to be scrambled: the $^{13}$C NMR spectrum at room temperature ($CD_2Cl_2$) shows the CO resonance at $\delta$ 199.8 as a sharp singlet.

## $[Ru_6C(CO)_{14}(NO)(C_3H_5)]$ 3

The solid-state structure of compound **3**, which we reported previously,[9] has the allyl and NO groups as shown. A 400 MHz $^1$H NMR spectrum measured at 203 K displayed two doublets due to non-equivalent *anti*-protons at $\delta$ −0.23 ($J = 12.3$) and 0.31 ($J = 12.4$ Hz), a multiplet for the central proton at $\delta$ 0.63, and a doublet and a singlet due to non-equivalent *syn*-protons at $\delta$ 2.96 ($J = 5.8$ Hz) and 4.04, respectively. The *anti* peaks coalesce at 253 K, the *syn* peaks at 263 K: both experimental and simulated spectra as a function of temperature are depicted in Fig. 3. The analysis of the kinetic data using the Eyring equation (Fig. 5) afforded the thermodynamic parameters $\Delta H^{\ddagger} = 9.5 \pm 0.1$ kcal mol$^{-1}$ and $\Delta S^{\ddagger} = -7.8 \pm 0.5$ cal K$^{-1}$ mol$^{-1}$.

The $^{13}$C NMR spectrum measured at room temperature in $(CD_3)_2CO$ showed a singlet peak for the CO ligands at $\delta$ 200.2.
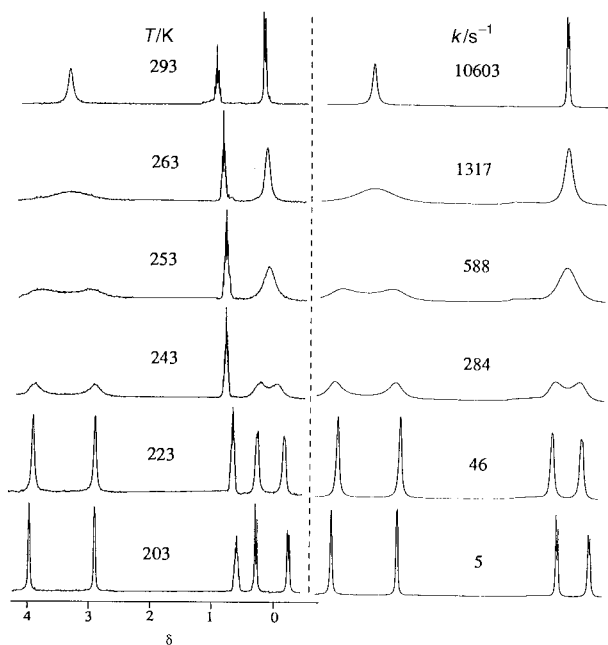
**Fig. 3** Variable-temperature $^1H$ NMR spectra (400 MHz) of the $C_3H_5$ region of compound **3** in [$^2H_8$]toluene. Left: observed spectra. Right: simulated spectra (*syn*- and *anti*-protons only) and rates



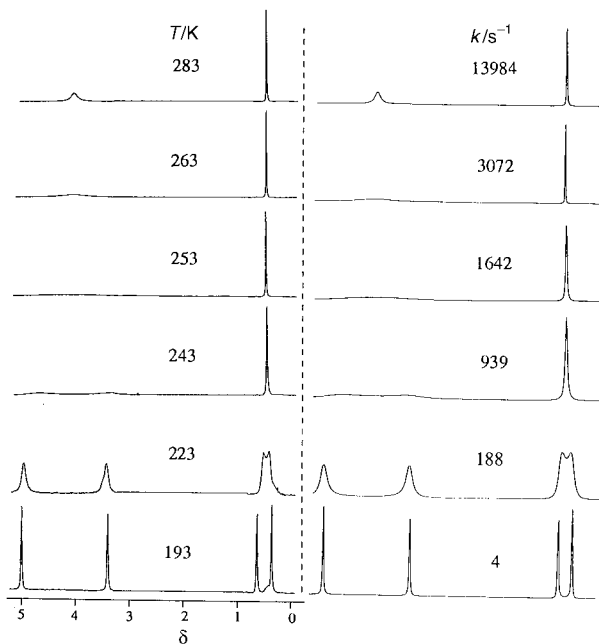**Fig. 5** Eyring plots of the dynamic processes of compounds **2** ($\bigcirc$), **3** ($\square$) and **4** ($\bullet$) as deduced from variable-temperature $^1H$ NMR spectroscopy



**Fig. 4** Variable-temperature $^1H$ NMR spectra (400 MHz) of the $C_3H_4$ region of compound **4** in [$^2H_8$]toluene. Left: observed spectra where the singlet peak of $CO_2Me$ at around $\delta$ 2.9 is omitted. Right: simulated spectra (*syn*- and *anti*-protons only) and rates
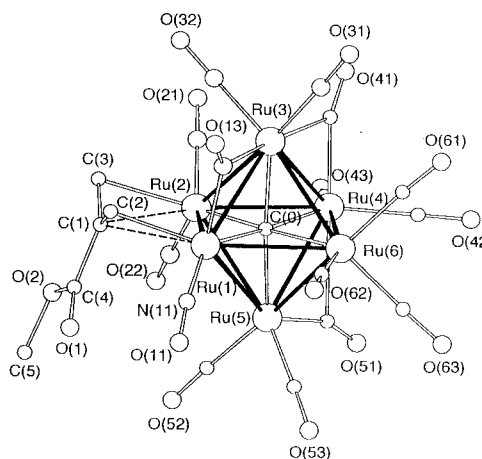


**Fig. 6** Perspective view and atom numbering scheme for complex **4**

## [Ru$_6$C(CO)$_{14}$(NO)(C$_3$H$_4$CO$_2$Me)] 4

In order to examine the mobility of the allyl ligand in allyl/NO complexes, we prepared complex **4** where the hydrogen on the central carbon of the allyl in **3** has been replaced with a $CO_2Me$ group. The $^1H$ NMR spectrum at 193 K exhibited *anti*-proton peaks at $\delta$ 0.29 (singlet) and 0.56 (doublet, $J = 3.9$ Hz), a methoxycarbonyl singlet at $\delta$ 2.85, and two *syn*-proton signals at $\delta$ 3.38 and 5.02. The variable-temperature $^1H$ NMR spectra of **4** measured in the temperature range 283–193 K were similar to those of **3** as shown in Fig. 4. The activation parameters determined by the spectral simulation were $\Delta H^{\ddagger} = 9.2 \pm 0.3$ kcal mol$^{-1}$ and $\Delta S^{\ddagger} = -7.1 \pm 1.4$ cal K$^{-1}$ mol$^{-1}$ (Fig. 5), which were virtually identical to the corresponding values for **3**.
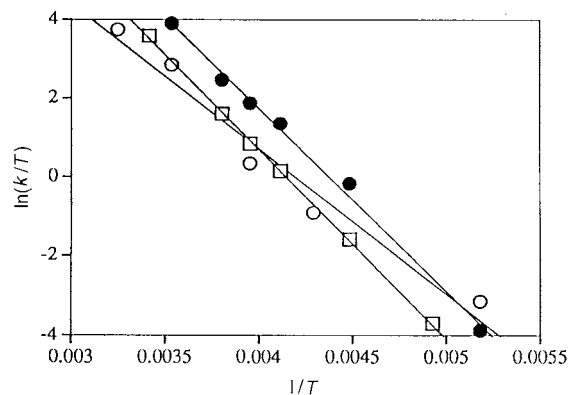
The crystal structure of compound **4** is shown in Fig. 6. The unit cell contains two independent molecules but since the structural parameters are quite similar to each other we refer to mean values of the two hereafter. The relative orientation of the NO and allyl ligands is identical to that in **3** but the number of CO bridges is different: three in **4** and only one in **3**. The potential-energy surface of the cluster is, therefore, flat as a function of the number of terminal and bridging CO ligands, which must be relevant to the easy scrambling of CO ligands in solution. The $CO_2Me$ group bonded to C(1) is bent away from the cluster core apparently for steric reasons and the dihedral angle between the allyl and ester planes is 21°.

Since the allyl central carbon C(1) lies on the plane defined by equatorial Ru(1)Ru(2)Ru(4)Ru(6) and C(0) (deviation from this plane 0.05 Å), and the allyl plane is almost perpendicular to this equatorial plane (dihedral angle 85°), one may take the C(0)–C(1) vector as the axis to examine the rotational motion of the allyl ligand. A computer graphic study indicated that when the allyl group is rotated by 90° around this axis the distance between the methoxycarbonyl carbon C(4) and Ru(2), or Ru(1) when turned in the other direction, becomes as short as 2.6 Å. Simple rotational movement of this allyl group at the edge of the cluster should thus be sterically quite difficult. Therefore the observed fluxionality, *i.e.* equivalence of two *syn*-protons at C(2) and C(3) as well as of two *anti*-protons on the same carbons, is explained by rapid migration of the NO (and CO) unit over the metal atoms in the cluster framework rather than by rotation of the allyl moiety. That the activation parameters are independent of the steric and electronic character of the allyl group, as observed in complexes **3** and **4**, strongly supports a stationary allyl group and hence a migrating NO unit. In ad-

dition, a non-migrating allyl is compatible with the mechanism for the SO$_2$/allyl complex **2** proposed based on the symmetry of the complex.

The $^1$H NMR spectrum of the $\mu$-allyl group is thus a convenient tool to monitor dynamic processes of other ligands in high-nuclearity clusters.

**Table 1** Crystallographic data for [Ru$_6$C(CO)$_{14}$(NO)(C$_3$H$_4$CO$_2$Me)] **4**

| | |
|---|---|
| Formula | C$_{20}$H$_7$NO$_{17}$Ru$_6$ |
| $M$ | 1139.69 |
| Crystal system | Triclinic |
| Space group | $P\bar{1}$ (no. 2) |
| $a$/Å | 16.834(6) |
| $b$/Å | 18.267(6) |
| $c$/Å | 9.776(4) |
| $\alpha$/° | 95.85(2) |
| $\beta$/° | 97.65(2) |
| $\gamma$/° | 100.27(2) |
| $U$/Å$^3$ | 2907(2) |
| $Z$ | 2 |
| $D_c$/g cm$^{-3}$ | 1.30 |
| Crystal size/mm | 0.47 × 0.18 × 0.10 |
| $F(000)$ | 1068 |
| $\mu$/cm$^{-1}$ | 15.301 |
| $2\theta_{max}$/° | 55 |
| No. data measured | 13 883 |
| No. unique data | 10 413 ($F \geqslant 3\sigma$) |
| No. parameters | 794 |
| Absorption correction | $\psi$ Scan |
| Transmission coefficients | 0.7810–0.9994 |
| Final $R$ | 0.0405 |
| Final $R'$ | 0.0424 |
| Goodness of fit | 3.26 |
| Maximum $\Delta/\sigma$ | 0.285 |
| $\Delta\rho$/e Å$^{-3}$ | 1.45 |

# Experimental

All manipulations were performed under an atmosphere of argon. The cluster compound [Ru$_6$C(CO)$_{14}$(NO)($\eta^3$-C$_3$H$_5$)] was prepared by the published procedure.[9] The NMR spectra were obtained on a JEOL GX-400 spectrometer. Line-shape analyses were performed using the program DNMR 5,[15] with the *syn*- and *anti*-protons but not the central proton of the allyl group simulated for the sake of simplicity.

### Synthesis of [Ru$_6$C(CO)$_{14}$(NO)(C$_3$H$_4$CO$_2$Me)] 4

A CH$_2$Cl$_2$ solution (10 cm$^3$) of [N(PPh$_3$)$_2$]$_2$[Ru$_6$C(CO)$_{16}$] (250 mg, 0.117 mmol) and methyl 2-(bromomethyl)acrylate (180 mg, 1 mmol) was placed in a stainless-steel pressure vessel equipped with an inner glass tube and heated at 85 °C for 2 h. The solvent was removed from the resulting solution under reduced pressure, and the residue worked up by silica gel column chromatography. Elution with benzene–CH$_2$Cl$_2$ (2:1 v/v) separated a red band. Evaporation of the eluate to dryness afforded [N(PPh$_3$)$_2$][Ru$_6$C(CO)$_{15}$(C$_3$H$_4$CO$_2$Me)] as a red-brown solid (144 mg, 73%). $^1$H NMR (CDCl$_3$): $\delta$ 0.30 (2 H, s, *anti*-H), 3.39 (3 H, s, Me), 4.19 (2 H, s, *syn*-H) and 7.4–7.7 [30 H, m, N(PPh$_3$)$_2$]. To a CH$_2$Cl$_2$ (5 cm$^3$) solution of [N(PPh$_3$)$_2$][Ru$_6$C-(CO)$_{15}$(C$_3$H$_4$CO$_2$Me)] (30 mg, 0.018 mmol) in a round-bottom flask (100 cm$^3$) was added NO gas (1.7 cm$^3$, 0.072 mmol) by a syringe. The solution immediately darkened. After stirring for 30 min at room temperature it was concentrated and chromatographed on silica gel. A brown band was eluted with hexane–benzene (2:1 v/v) and the eluate was concentrated. Crystallization from benzene–hexane yielded reddish brown crystals of compound **4** (20% yield). IR (CH$_2$Cl$_2$): 2113w, 2087m, 2047s, 1995w, 1849w and 1770w cm$^{-1}$. $^1$H NMR ([$^2$H$_8$]toluene, room temperature, 270 MHz): $\delta$ 0.60 (2 H, d, $J$ = 3.6 Hz,

**Table 2** Selected bond lengths (Å) and angles (°) for complex **4**

| | Molecule 1 | Molecule 2 | | Molecule 1 | Molecule 2 |
|---|---|---|---|---|---|
| Ru(1)–Ru(2) | 2.9569(13) | 2.9604(13) | Ru(1)–C(2) | 2.156(9) | 2.157(11) |
| Ru(1)–Ru(3) | 2.8283(14) | 2.8283(14) | Ru(2)–C(1) | 2.504(8) | 2.494(9) |
| Ru(1)–Ru(5) | 2.9802(13) | 3.0008(13) | Ru(2)–C(3) | 2.217(9) | 2.202(10) |
| Ru(1)–Ru(6) | 2.8965(12) | 2.8855(13) | Ru(1)–N(11) | 1.749(6) | 1.774(9) |
| Ru(2)–Ru(3) | 2.9283(13) | 2.9268(14) | Ru(1)–C(13) | 2.039(9) | 2.052(8) |
| Ru(2)–Ru(4) | 2.8441(12) | 2.8568(12) | Ru(3)–C(13) | 2.165(8) | 2.120(10) |
| Ru(2)–Ru(5) | 2.9262(13) | 2.9131(13) | Ru(3)–C(41) | 2.301(9) | 2.382(10) |
| Ru(3)–Ru(4) | 2.8771(14) | 2.8599(13) | Ru(4)–C(41) | 2.021(9) | 1.986(8) |
| Ru(3)–Ru(6) | 2.8667(13) | 2.8940(14) | Ru(4)–C(51) | 2.572(11) | 2.650(8) |
| Ru(4)–Ru(5) | 2.8918(14) | 2.8972(13) | Ru(5)–C(51) | 1.928(9) | 1.922(10) |
| Ru(4)–Ru(6) | 2.8789(13) | 2.8937(13) | C(1)–C(2) | 1.443(11) | 1.464(14) |
| Ru(5)–Ru(6) | 2.8642(13) | 2.8327(14) | C(1)–C(3) | 1.420(10) | 1.423(13) |
| Ru(1)–C(0) | 2.032(7) | 2.047(7) | C(1)–C(4) | 1.505(12) | 1.540(11) |
| Ru(2)–C(0) | 2.026(6) | 2.023(7) | O(11)–N(11) | 1.162(9) | 1.147(12) |
| Ru(3)–C(0) | 2.060(7) | 2.041(6) | O(13)–C(13) | 1.158(11) | 1.167(12) |
| Ru(4)–C(0) | 2.060(7) | 2.060(7) | O(41)–C(41) | 1.147(10) | 1.145(11) |
| Ru(5)–C(0) | 2.039(7) | 2.049(6) | O(51)–C(51) | 1.140(12) | 1.154(12) |
| Ru(6)–C(0) | 2.071(7) | 2.069(7) | Ru–C* | 1.877(10)–1.924(11) | 1.873(11)–1.912(10) |
| Ru(1)–C(1) | 2.701(7) | 2.696(9) | O–C* | 1.122(13)–1.149(15) | 1.110(15)–1.150(14) |
| | | | | | |
| Ru(2)–Ru(1)–C(1) | 52.3(2) | 52.1(2) | C(2)–C(1)–C(4) | 114.4(7) | 120.6(8) |
| Ru(2)–Ru(1)–C(2) | 79.8(2) | 80.3(3) | C(3)–C(1)–C(4) | 121.0(7) | 114.1(8) |
| Ru(1)–Ru(2)–C(1) | 58.6(2) | 58.5(2) | Ru(1)–C(2)–C(1) | 95.2(5) | 94.3(6) |
| Ru(1)–Ru(2)–C(3) | 88.2(2) | 88.4(3) | Ru(2)–C(3)–C(1) | 84.0(5) | 84.0(6) |
| C(1)–Ru(2)–C(3) | 34.3(2) | 34.6(3) | Ru(1)–C(13)–Ru(3) | 84.5(3) | 85.4(4) |
| Ru(1)–N(11)–O(11) | 172.5(8) | 172.9(9) | Ru(1)–C(13)–O(13) | 139.4(7) | 137.1(8) |
| Ru(1)–C(1)–Ru(2) | 69.1(2) | 69.4(2) | Ru(3)–C(13)–O(13) | 136.0(7) | 137.6(7) |
| Ru(1)–C(1)–C(2) | 52.6(4) | 52.9(5) | Ru(3)–C(41)–Ru(4) | 83.2(3) | 81.3(3) |
| Ru(1)–C(1)–C(3) | 120.9(6) | 121.1(6) | Ru(3)–C(41)–O(41) | 130.6(7) | 128.4(7) |
| Ru(1)–C(1)–C(4) | 104.7(5) | 109.5(6) | Ru(4)–C(41)–O(41) | 146.0(8) | 150.3(8) |
| Ru(2)–C(1)–C(2) | 112.7(6) | 113.3(6) | Ru(4)–C(51)–Ru(5) | 78.6(3) | 76.8(3) |
| Ru(2)–C(1)–C(3) | 61.7(4) | 61.4(5) | Ru(4)–C(51)–O(51) | 124.4(7) | 122.4(7) |
| Ru(2)–C(1)–C(4) | 100.0(5) | 107.0(5) | Ru(5)–C(51)–O(51) | 157.1(9) | 160.8(7) |
| C(2)–C(1)–C(3) | 122.5(8) | 122.9(7) | Ru–C–O* | 175.5(8)–179.4(9) | 173.5(11)–179.1(8) |

\* Terminal carbonyl ligands.

*anti*-H), 3.01 (3 H, s, Me) and 4.41 (2 H, br s, *syn*-H) (Found: C, 21.1; H, 0.6; N, 1.2. Calc. for $C_{20}H_7NO_{17}Ru_6$: C, 21.1; H, 0.6; N, 1.25%).

### Crystallography

Deep red crystals of compound **4** were obtained by addition of hexane to a $CH_2Cl_2$ solution of it followed by concentration. One was fixed with Apiezon grease L in a glass capillary under argon. Intensity data were collected at 21 °C on an Enraf-Nonius CAD 4 four-circle automated diffractometer with graphite-monochromatized Mo-Kα radiation (λ 0.710 73 Å). Crystal data and experimental details are given in Table 1. A survey of the data set revealed no systematic extinctions and no symmetry other than the Friedel condition ($\bar{1}$). Thus, the crystal belongs to the triclinic class with space group $P1$ or $P\bar{1}$. The latter centrosymmetric possibility was strongly indicated by the cell volume (consistent with $Z = 2$) and confirmed by successful refinement of the structure for this low-symmetry space group. Data were corrected for absorption.[16] The analytical form of the scattering factor[17] for the appropriate neutral atom was corrected for both real ($Df'$) and imaginary ($Df''$) components of the anomalous dispersion.[18] The structure was solved by direct methods, MULTAN,[19] which located twelve ruthenium atoms of the asymmetric unit. All the non-hydrogen atoms were located from subsequent Fourier-difference syntheses, and refined by the block-diagonal least-squares method (based on $F$)[20] with anisotropic thermal parameters for all atoms. The hydrogen atoms were not located. Assignment of the NO ligand was made from the shorter bond length to the ruthenium atom compared with those of CO. Replacement of a nitrogen with a carbon atom led to marginally higher residuals and goodness of fit. The final $R(F)$ and $R'(F)$ values were 0.041 and 0.042 with the weighting scheme $w = 1$. The final Fourier-difference synthesis showed no unexpected features, with the highest peak 1.45 e Å$^{-3}$ within the covalent radius of Ru(2) (0.78 Å). The unit cell contains two crystallographically unique but virtually the same clusters. Selected bond lengths and angles are listed in Table 2.

Atomic coordinates, thermal parameters, and bond lengths and angles have been deposited at the Cambridge Crystallographic Data Centre (CCDC). See Instructions for Authors, *J. Chem. Soc., Dalton Trans.*, 1997, Issue 1. Any request to the CCDC for this material should quote the full literature citation and the reference number 186/341.

### References

1 J. L. Vidal, W. E. Walker and R. C. Schoening, *Inorg. Chem.*, 1981, **20**, 238; A. Fumagalli, S. Martinengo, G. Ciani, A. Sironi and B. T. Heaton, *J. Chem. Soc., Dalton Trans.*, 1988, 163; S. R. Drake, B. F. G. Johnson and J. Lewis, *J. Chem. Soc., Dalton Trans.*, 1988, 1517; A. Fumagalli, R. D. Pergola, F. Bonacina, L. Garlaschelli, M. Moret and A. Sironi, *J. Am. Chem. Soc.*, 1989, **111**, 165; B. F. G. Johnson, R. Khatta, J. Lewis, P. R. Raithby and M. J. Rosales, *J. Organomet. Chem.*, 1990, **385**, 387; A. Fumagalli, S. Martinengo, G. Ciani, M. Moret and A. Sironi, *Inorg. Chem.*, 1992, **31**, 2900; S. P. Tunik, V. R. Krym, G. L. Starova, A. B. Nikol'skii, I. S. Podkorytov, S. Ooi, M. Yamasaki and M. Shiro, *J. Organomet. Chem.*, 1994, **481**, 83; B. F. G. Johnson, J. Lewis, H. Curtis, T. Adatia, M. McPartlin and J. Morris, *J. Chem. Soc., Dalton Trans.*, 1994, 243; T. Blum, M. P. Brown, B. T. Heaton, A. S. Hor, J. A. Iggo, J. S. Z. Sabounchei and A. K. Smith, *J. Chem. Soc., Dalton Trans.*, 1994, 513; C.-J. Su, Y. Chi, S.-M. Peng and G.-H. Lee, *Organometallics*, 1995, **14**, 4286.
2 C. J. Brown, P. J. McCarthy and I. D. Salter, *J. Chem. Soc., Dalton Trans.*, 1990, 3583.
3 S. R. Drake, B. F. G. Johnson and J. Lewis, *J. Organomet. Chem.*, 1988, **340**, C31; A. Fumagalli, S. Martinengo, V. G. Albano, D. Braga and F. Grepioni, *J. Chem. Soc., Dalton Trans.*, 1989, 2343; C.-C. Chen, Y. Chi, S.-M. Peng and G.-H. Lee, *J. Chem. Soc., Dalton Trans.*, 1993, 1823; C. E. Housecroft, D. M. Matthews, A. Waller, A. J. Edwards and A. L. Rheingold, *J. Chem. Soc., Dalton Trans.*, 1993, 3059.
4 S. A. R. Knox, B. R. Lloyd, D. A. V. Morton, S. M. Nicholls, A. G. Orpen, J. M. Viñas, M. Weber and G. K. Williams, *J. Organomet. Chem.*, 1990, **394**, 385.
5 C. J. Adams, M. I. Bruce, M. Schulz, B. W. Skelton and A. H. White, *J. Organomet. Chem.*, 1994, **472**, 285.
6 A. J. Blake, A. H. Harrison, B. F. G. Johnson, E. J. L. McInnes, S. Parsons, D. S. Shephard and L. J. Yellowlees, *Organometallics*, 1995, **14**, 3160.
7 J. Washington and J. Takats, *Organometallics*, 1990, **9**, 925; L. J. Farrugia and S. E. Rae, *Organometallics*, 1992, **11**, 196; C. P. Casey, R. A. Windenhoefer, S. L. Hallenbeck, R. K. Hayashi and J. A. Gavney, jun., *Organometallics*, 1994, **13**, 4720; D. Wang, H. Shen, M. G. Richmond and M. Schwartz, *Organometallics*, 1995, **14**, 3636.
8 T. Inui, S. Iwamoto and S. Shimizu, *Proc. 9th Int. Zeolite Conf.*, 1992, **II**, 405.
9 T. Chihara, K. Sawamura, H. Ikezawa, H. Ogawa and Y. Wakatsuki, *Organometallics*, 1996, **15**, 415.
10 T. Chihara, K. Sawamura, H. Ogawa and Y. Wakatsuki, *J. Chem. Soc., Chem. Commun.*, 1994, 1179.
11 T. Chihara and Y. Wakatsuki, unpublished work.
12 P. L. Bogdan, M. Sabat, S. A. Sunshine, C. Woodcock and D. F. Shriver, *Inorg. Chem.*, 1988, **27**, 1904.
13 G. J. Kubas, *Acc. Chem. Res.*, 1994, **27**, 183.
14 G. B. Karet, C. L. Stern, D. M. Norton and D. F. Shriver, *J. Am. Chem. Soc.*, 1993, **113**, 9979.
15 D. S. Stephenson and G. Binsch, *Quantum Chemistry Program Exchange*, 1978, **10**, 365.
16 A. C. T. North, D. C. Phillips and F. S. Mathews, *Acta Crystallogr., Sect. A*, 1968, **24**, 351.
17 D. T. Cromer and J. T. Waber, in *International Tables for X-Ray Crystallography*, eds. J. A. Ibers and W. C. Hamilton, Kynoch Press, Birmingham, 1974, vol. 4, p. 71.
18 D. T. Cromer, in *International Tables for X-Ray Crystallography*, eds. J. A. Ibers and W. C. Hamilton, Kynoch Press, Birmingham, 1974, vol. 4, p. 148.
19 P. Main, S. E. Hull, L. Lessinger, G. Germain, J.-P. Declerq and M. M. Woolfson, MULTAN 78, University of York, 1978.
20 T. Sakurai and K. Kobayashi, *Rikagaku Kenkyusho Hokoku*, 1979, **55**, 69.